ELSEVIER

Electric Power Systems Research, 29 (1994) 161-169

ELECTRIC POWER SYSTEMS RESEARCH

An accurate fault location algorithm using synchronized sampling

M. Kezunović and J. Mrkić

Texas A&M University, College Station, TX 77843, USA

B. Peruničić

Lamar University, Beaumont, TX 77710, USA

(Received November 5, 1993)

Abstract

This paper introduces new fault location algorithms based on synchronized sampling. A time domain model of a transmission line is used as a basis for the algorithm development. Samples of voltages and currents at the ends of a transmission line are taken synchronously and used to calculate fault location. The paper discusses two different algorithm forms utilizing two line models. A number of tests are performed using EMTP simulations of faults. The algorithm results show high accuracy while the computational burden is moderate.

Keywords: Fault location; Time domain models; Synchronized sampling; EMTP simulations

Introduction

Fault location on transmission lines is a very well-known problem which has been studied for a long time [1-3]. Introduction of microprocessors to the field of power system monitoring and control has initiated extensive research on digital algorithms for fault location. As a result, a variety of different approaches have been introduced [4-15]. The main differences between various algorithms defined so far are in the models used, data required and errors introduced when calculating fault location.

In the past, the most common approach was to model transmission lines using phasors. This approach is based on calculation of the apparent line impedance using data from either one or all transmission line ends. If data from only one end are used, then the number of unknowns is larger than the number of equations. This problem was solved by making various assumptions such as: the fault resistance is zero [4]; the fault resistance has a real part only [5, 6]; the ratio of the fault currents from two line ends is a real number [6]; the ratio of the fault currents is determined using knowledge about source impedances [6]. When the measurements from two ends are available, the number of equations is sufficient to find the location of the fault. When the sampling at two ends is synchronized, the calculations are rather simple [7, 8]. If the sampling is not synchronized, then nonlinear equations have to be solved and increased computational burden is introduced [8, 9]. The phasor approach is quite attractive as long as all of the algorithm assumptions are met and the phasor quantities are estimated accurately.

Another approach is based on the use of the Laplace and the Fourier transforms [10, 11]. This technique is based on the superposition theorem and again introduces several assumptions regarding fault resistance and current ratios. Here also, the results obtained are quite accurate as long as the assumptions are satisfied.

The traveling wave approach was also studied [12-15]. This approach is based either on the travel time measurements using correlation techniques [12] or on the reconstruction of voltages and currents at the fault location [13-15]. The traveling wave techniques offer some advantages but the computational complexity is increased.

Finally, a time domain representation of a transmission line model has also been considered [16]. The model is obtained using Laplace and Z transforms. Data samples are considered as being available from one end only. The voltage at the other end is estimated using prefault data.

SSDI 0378-7796(94)00826-P

The time domain approach to fault location is utilized in this paper to achieve extreme accuracies by using samples at both ends of a transmission line. Two different algorithm forms are developed for short and long transmission line applications. Since the synchronized sampling technology is becoming affordable and reliable [17–19], it is demonstrated that this new approach has some important advantages over those introduced so far.

The main advantage of the new approach is its rather simple requirement that only the line model and the samples at the two ends of a transmission line need to be known for algorithm implementation. Model characteristics and operating conditions in the rest of the system do not need to be known. Operating conditions on the line of interest can also be highly unbalanced, even including conditions where some of the phases are deenergized. An inductive component of fault inductance many be present and the fault resistance may be variable in time. Fault waveforms may be arbitrary, containing any number of nonfundamental frequency components. Data sampling requirements are almost arbitrary, only requiring samples to be synchronized and taken at a sufficiently high sampling rate to provide adequate approximation of the derivatives. Line transposition does not significantly affect the results. The influence of mutual coupling can be taken into account if synchronized samples from the corresponding ends of the parallel lines are made available. Finally, the new algorithms provide very reliable fault detection and fault classification, which may be useful in some more elaborate fault analysis applications. Last, but not least, the new approach provides very good accuracy, as good as in some of the 'best' approaches proposed so far, and in many instances even better. All of the mentioned advantages indicate that the new approach provides fault location that is indeed robust and, as such, may be more practical than some of the other schemes proposed so far.

Theoretical background

The principles of the technique using the synchronized phase voltage and current samples at both ends of the transmission line to calculate the location of the fault on any line are presented in this section.

Consider the arbitrary unfaulted three-phase system depicted in Fig. 1. The two ends of the transmission line of interest are labeled S and R. The transmission line connects two parts of the system, labeled subsystem 1 and subsystem 2. The vectors of the phase voltages and currents at the two ends of the transmission line are $\boldsymbol{v}_S$, $\boldsymbol{i}_S$, and $\boldsymbol{v}_R$, $\boldsymbol{i}_R$, respectively. The length of the line is d. At any location X along the given line, the instantaneous values of the phase voltages and currents are

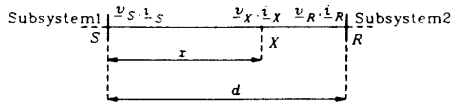

Fig. 1. Unfaulted three-phase system.

related through the linear partial differential equations:

$$\frac{\partial \boldsymbol{v}(x,t)}{\partial x} = -\mathbf{r}\boldsymbol{i}(x,t) - \mathbf{l}\frac{\partial \boldsymbol{i}(x,t)}{\partial t}$$
$$\frac{\partial \boldsymbol{i}(x,t)}{\partial x} = -\mathbf{g}\boldsymbol{v}(x,t) - \mathbf{c}\frac{\partial \boldsymbol{v}(x,t)}{\partial t} \quad (1)$$

where **r**, **l**, **g**, and **c** are matrices of line parameters per unit length, that is, resistance, inductance, conductance, and capacitance, respectively. x is the distance between the point X and the end S of the transmission line. $\boldsymbol{v}_X$ and $\boldsymbol{i}_X$ are vectors of the instantaneous phase voltages and currents at point X of the line, defined as

$$\boldsymbol{v}_X = \boldsymbol{v}(x,t) = [v_a(x,t), v_b(x,t), v_c(x,t)] \quad (2)$$

$$\boldsymbol{i}_X = \boldsymbol{i}(x,t) = [i_a(x,t), i_b(x,t), i_c(x,t)] \quad (3)$$

In the case of a homogeneous line (constant line parameters per unit length), the solution of the system of equations (1) relates the phase voltages and currents of any two points along the line. Thus, the voltages and currents at the end S can be expressed in terms of the voltages and currents at the end R (and vice versa) as

$$\boldsymbol{v}_R = L^v\{\boldsymbol{v}_S, \boldsymbol{i}_S, d\} \quad (4)$$

$$\boldsymbol{i}_R = L^i\{\boldsymbol{v}_S, \boldsymbol{i}_S, d\} \quad (5)$$

$\boldsymbol{v}_S$, $\boldsymbol{i}_S$, and $\boldsymbol{v}_R$, $\boldsymbol{i}_R$ are vectors defined in the same manner as $\boldsymbol{v}_X$, $\boldsymbol{i}_X$ (eqns. (2) and (3)). L^v and L^i are linear operators with respect to the vectors of voltages $\boldsymbol{v}$ and currents $\boldsymbol{i}$.

The relations between voltages and currents at any two points on the transmission line (eqns. (4) and (5)) are not influenced by the configuration nor the parameters of the rest of the system of which the line is a part. On the other hand, these relations depend on the unit length line parameters (**r**, **l**, **g**, **c**), and the line length (d); this dependence is not necessarily linear. The particular form of the operators L^v and L^i depends on the transmission line parameters and its electrical length.

Now, consider the faulted three-phase transmission line depicted in Fig. 2. The fault point is denoted as F, and is at a distance x from the line end R.

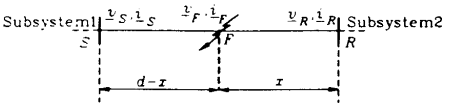

Fig. 2. Faulted three-phase transmission line.

Due to a fault occurrence at the point F, the transmission line is divided into two homogeneous parts: one is between the end S and the fault point F, and the other one is between the end R and F. At any point on the line between S and F the voltages can be expressed in terms of the end S voltages and currents only. Similarly, at any point on the line between R and F the voltages can be expressed in terms of the end R voltages and currents only. Therefore, the point F on the faulted line is the unique location at which the phase voltages $\boldsymbol{v}_F$ can be expressed in terms of both line ends' voltages and currents (eqns. (4) and (5)).

The phase voltages at the fault point F are related to both line ends' phase voltages and currents (eqn. (4)):

$$\boldsymbol{v}_F = L^v\{\boldsymbol{v}_S, \boldsymbol{i}_S, d-x\} \tag{6}$$

$$\boldsymbol{v}_F = L^v\{\boldsymbol{v}_R, \boldsymbol{i}_R, x\} \tag{7}$$

where $\boldsymbol{v}_F$ is the vector of instantaneous phase voltages defined in the same way as $\boldsymbol{v}_X$ (eqn. (2)), and $d-x$ is the distance between end S and the fault point F.

Because of the continuity of the voltage along the transmission line, eqns. (6) and (7) can be combined, leading to

$$L^v\{\boldsymbol{v}_S, \boldsymbol{i}_S, d-x\} = L^v\{\boldsymbol{v}_R, \boldsymbol{i}_R, x\} \tag{8}$$

Finally, consider a hypothetical unfaulted three-phase transmission line having the same characteristics as the faulted one. This line is depicted in Fig. 3. The point F on this hypothetical unfaulted line is at the same location as the fault point F on the faulted line (Fig. 2). The vectors of phase voltages and currents of the hypothetical line are defined as for the case of the faulted line.

Let us assume that the vectors of voltages and currents at the end S of the hypothetical line are exactly the same as the corresponding ones $\boldsymbol{v}_S$ and $\boldsymbol{i}_S$ on the actual faulted line. Therefore, at the point F on the hypothetical line the voltages are the same as the corresponding ones on the faulted line. Since the hypothetical line is unfaulted, it is homogeneous over its whole length. Therefore, the end R voltages and currents on the hypothetical line can be expressed, using eqns. (4) and (5), as

$$\tilde{\boldsymbol{v}}_R = L^v\{\boldsymbol{v}_S, \boldsymbol{i}_S, d\} \tag{9}$$

$$\tilde{\boldsymbol{i}}_R = L^i\{\boldsymbol{v}_S, \boldsymbol{i}_S, d\} \tag{10}$$

The parts of the hypothetical line between the end S and F and the end R and F are also homogeneous. Thus, for the point F, expression (8) becomes

$$L^v\{\boldsymbol{v}_S, \boldsymbol{i}_S, d-x\} = L^v\{\tilde{\boldsymbol{v}}_R, \tilde{\boldsymbol{i}}_R, x\} \tag{11}$$

Due to the assumption that the end S voltages and currents are the same on both the faulted and hypothetical lines, eqns. (8) and (11) can be combined, leading to

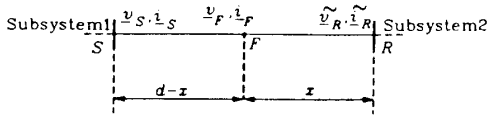

Fig. 3. Hypothetical three-phase transmission line.

$$L^v\{\boldsymbol{v}_R, \boldsymbol{i}_R, x\} - L^v\{\tilde{\boldsymbol{v}}_R, \tilde{\boldsymbol{i}}_R, x\} = 0 \tag{12}$$

The linearity of operators L^v and L^i with respect to the vectors of voltages and currents enables expression (12) to be rewritten as

$$L^v\{\Delta\boldsymbol{v}_R, \Delta\boldsymbol{i}_R, x\} = 0 \tag{13}$$

where $\Delta\boldsymbol{v}_R$ and $\Delta\boldsymbol{i}_R$ are defined as

$$\Delta\boldsymbol{v}_R = \boldsymbol{v}_R - \tilde{\boldsymbol{v}}_R$$

$$\Delta\boldsymbol{i}_R = \boldsymbol{i}_R - \tilde{\boldsymbol{i}}_R$$

Equation (13) is the *generic fault location equation*. It relates the unknown distance x to the fault point F and the mismatch of the phase voltages and currents, $\Delta\boldsymbol{v}_R$ and $\Delta\boldsymbol{i}_R$. The mismatches $\Delta\boldsymbol{v}_R$ and $\Delta\boldsymbol{i}_R$ contain both line ends' voltage and current values. While $\boldsymbol{v}_R$ and $\boldsymbol{i}_R$ are the measured vectors at one end, $\tilde{\boldsymbol{v}}_r$ and $\tilde{\boldsymbol{i}}_R$ are the calculated ones. The vectors $\tilde{\boldsymbol{v}}_R$ and $\tilde{\boldsymbol{i}}_R$ are calculated using the measured values of the other line end, $\boldsymbol{v}_S$ and $\boldsymbol{i}_S$ (eqns. (9) and (10)). Therefore, the generic equation (13) implicitly relates the unknown distance x to the fault point F, and both line ends' instantaneous phase voltages and currents, $\boldsymbol{v}_S$, $\boldsymbol{i}_S$ and $\boldsymbol{v}_R$, $\boldsymbol{i}_R$.

For a particular transmission line, the generic equation (13) has a unique form that determines the way it can be solved for an unknown fault location. Here, the derivation of the explicit fault location equation in the case of a short line will be given first. Then, the derivation and the indirect way of solving the generic equation (13) in the case of a long line will be presented. The short-line model is suitable when the conductance and capacitance to earth may be neglected. The long-line model is adequate for lines with low losses having very small resistance and conductance. Most of the published literature considers short lines as being up to 50 miles long and long lines as over 150 miles.

Short-line application

This section presents the derivation of the fault location equation for the short transmission line, starting from the generic equation (13). Consider the short three-phase transmission line depicted in Fig. 4. The parts of the system connected to the ends of the line are

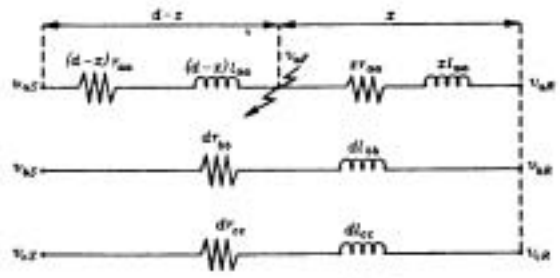

Fig. 4. Faulted short three-phase transmission line.

omitted in this Figure. The fault point F is at a distance x from the line end R, and d is the total line length.

In the case of the short transmission line, the line is commonly represented as the serial connection of an inductance and a resistance since the parallel line capacitance and conductance are negligible. It is assumed that the line is homogeneous over its whole length, and that it has constant parameters per unit length (Fig. 4):
self (phase) resistance: r_{aa}, r_{bb}, r_{cc}
mutual resistance: r_{ab}, r_{ac}, r_{bc}
self (phase) inductance: l_{aa}, l_{bb}, l_{cc}
mutual inductance: l_{ab}, l_{ac}, l_{bc}
No other assumptions about the transmission line are needed.

For such a transmission line, the generic fault location equation (13) becomes a system of three equations:

$$v_{mS}(t) - v_{mR}(t) - d\sum_{p=a,b,c}\left[r_{mp}i_{pS}(t) + l_{mp}\frac{di_{pS}(t)}{dt}\right] + x\sum_{p=a,b,c}\left[r_{mp}i_{pR}(t) + r_{mp}i_{pS}(t) + l_{mp}\frac{di_{pR}(t)}{dt} + l_{mp}\frac{di_{pS}(t)}{dt}\right] = 0 \qquad m = a, b, c \tag{14}$$

Since the phase voltage and current at both ends of the line are available in the sampled form, the system of fault location equations (14) can be rewritten in discrete form as

$$A_m(k) + B_m(k)x = 0 \tag{15}$$

where $A_m(k)$ and $B_m(k)$ for $m = a, b, c$ and $k = 1, 2, \ldots, N$ are defined as

$$A_m(k) = v_{mS}(k) - v_{mR}(k) - d\sum_{p=a,b,c}\left[\left(r_{mp} + \frac{l_{mp}}{\Delta t}\right)i_{pS}(k) - \frac{l_{mp}}{\Delta t}i_{pS}(k-1)\right] \tag{16}$$

$$B_m(k) = \sum_{p=a,b,c}\left\{\left(r_{mp} + \frac{l_{mp}}{\Delta t}\right)[i_{pR}(k) + i_{pS}(k)] - \frac{l_{mp}}{\Delta t}[i_{pR}(k-1) + i_{pS}(k-1)]\right\} \tag{17}$$

In eqns. (16) and (17), $v_{mS}(k)$ and $v_{mR}(k)$ are phase ($m = a, b, c$) voltage samples taken at the time instant $t = k\,\Delta t$ ($k = 1, 2, \ldots, N$) at the line ends S and R, respectively. Similarly, $i_{mS}(k)$ and $i_{mR}(k)$ are phase current samples taken at the time $t = k\,\Delta t$ at the line ends S and R. Δt is the sampling step and N is the total number of samples considered.

The system of fault location equations given by expression (15) is overspecified since it has just one unknown variable, distance x to the fault point. Therefore, the unknown distance x is determined using the *least-square estimate* for all three phases of the line together:

$$x = \frac{-\sum_{m=a,b,c}\sum_{k=1}^{N} A_m(k)\,B_m(k)}{\sum_{m=a,b,c}\sum_{k=1}^{N} B_m^2(k)} \tag{18}$$

Expression (18) is the fault location equation that defines the fault location algorithm for the short three-phase transmission line. This expression is simple and valid for any system operating conditions. Also, it does not depend on the type of fault, nor on the fault resistance.

Long-line application

This section describes an algorithm for solving the generic fault location equation (13) in the case of a long transmission line. For the short transmission line, the generic fault location expression has the form that enables explicit calculation of the distance x to the fault point (eqn. (18)). In the case of a long transmission line, the system of equations (1) has a solution that does not allow the derivation of an explicit fault location equation.

The line considered is a lossless single-phase long transmission line. Then, the system of differential equations (1) becomes a pair of partial differential equations:

$$\frac{\partial v(x,t)}{\partial x} = -l\frac{\partial i(x,t)}{\partial t} \tag{19}$$

$$\frac{\partial i(x,t)}{\partial x} = -c\frac{\partial v(x,t)}{\partial t} \tag{20}$$

Using the traveling wave approach, the solution of eqns. (19) and (20) has the form of Bergeron's equations (Appendix A). Thus, eqns. (4) and (5) that relate

the voltages and currents of the two ends of the homogeneous line become

$$v_R(t) = \frac{z}{2}[i_S(t-\tau) - i_X(t+\tau)] - \frac{1}{2}[v_X(t-\tau) + v_S(t+\tau)] \quad (21)$$

$$i_R(t) = -\frac{1}{2}[i_S(t-\tau) + i_S(t+\tau)] - \frac{1}{2z}[v_S(t-\tau) - v_S(t+\tau)] \quad (22)$$

where v_R and i_R correspond to end R of the line, and $v_S(t)$ and $i_S(t)$ correspond to end S of the line. z is the surge impedance of the line and τ is the surge traveling time, defined as

$$z = (l/c)^{1/2} \quad (23)$$

$$\tau = d(lc)^{1/2} \quad (24)$$

It can be seen that in eqns. (21) and (22) the distance does not appear explicitly; it is hidden in the surge traveling time τ. Furthermore, τ does not appear as the variable of eqns. (21) and (22), but as the value on which the voltage and current depend. Physically, eqns. (21) and (22) have the following meaning: to calculate the voltage and current at any point of the line, the 'forward' and 'backward' waveforms of the current and voltage of the other point are needed, and they are a function of the distance. Therefore, an explicit fault location equation for the long transmission line cannot be derived from the generic equation (13). Instead, an indirect method is used to solve the fault location equation in this case.

Above, the traveling wave approach was briefly introduced for the case of the long single-phase line. In the case of the three-phase line, the modal transform (Appendix A) is applied to decouple the system of equations (1). This enables the traveling wave procedure to be applied on each of the three modes, leading to Bergeron's equations for the three-phase line. In defining the algorithm for the long transmission line, only mode-1 signals are considered.

The generic fault location equation (13) combined with the long-line equations (21) and (22) leads to the expression

$$L^v\{\Delta v_R, \Delta i_R, x\} = \frac{z}{2}[\Delta i_R(t - vx) - \Delta i_R(t + vx)] + \frac{1}{2}[\Delta v_R(t - vx) + \Delta v_R(t + vx)] = 0 \quad (25)$$

where $v = (lc)^{1/2}$.

The following is a discrete version of eqn. (25):

$$L^v\{\Delta v_{Rn}, \Delta i_{Rn}, x\} = \frac{z}{2}[\Delta i_{R,\,n-m} - \Delta i_{R,\,n-m}] + \frac{1}{2}[\Delta v_{R,\,n-m} + \Delta v_{R,\,n-m}] = 0 \quad (26)$$

where

$\Delta i_{Rn} = \Delta i_R(n\ \Delta t)$ $\quad m\ \Delta t = vx$

$\Delta v_{Rn} = \Delta v_R(n\ \Delta t)$ $\quad m, n =$ integer

Equation (26) is available for each sample. Since there is only one unknown x, the system of equations is again overspecified. The best estimate may be found based on the minimum least-square estimate technique.

In this particular case, the criterion to be minimized is

$$J(x) = \sum_{n=0}^{N} [L^v(\Delta v_{Rn}, \Delta i_{Rn}, m)]^2 \quad (27)$$

Since the criterion is not linearly dependent on m, the search for a minimum has to be performed in an approximate way. First, several tentative values of m are selected using the short-line algorithm. The value of the criterion defined by eqn. (27) is calculated for these tentative values of m. The calculated values are used to make an approximation of the criterion function using a parabola. The minimum of this parabola determines the final value of m for which the corresponding fault location is determined.

The algorithm for the long transmission line involves some additional computations when compared with that for the short line. Nevertheless, it is again valid for any line operating conditions, and it does not depend on the type of fault, nor the fault resistance.

Performance evaluation

The performances of both the short- and long-line algorithms were evaluated using EMTP generated data [20]. Two test systems were modeled using the EMTP, one for testing the short-line algorithm, the other for testing the long-line algorithm. Both test systems are models of actual power systems. Test system 1 is a 161 kV power system with a short transmission line used for testing the short-line fault location algorithm. The transmission line considered is fully transposed and 13.35 miles long. The one-line diagram of system 1 is shown in Fig. 5; the transmission line of interest is that between buses 2 and 3. Data for the EMTP model of system 1 are given in Appendix B.

The other test system (system 2) is 345 kV with a long transmission line considered for testing the fault location algorithm for the long lines. The transmission line of interest is untransposed and 195 miles long. The one-line diagram of system 2 is shown in Fig. 6; the transmission line of interest is between buses 1 and 2. Data for the EMTP model of system 2 are also given in Appendix B.

It is interesting to note that the lines used for simulation have one unusual feature: the short line is trans-

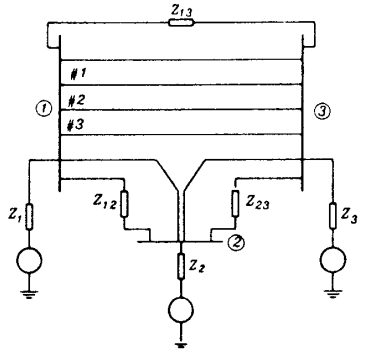

Fig. 5. One-line diagram of system 1.

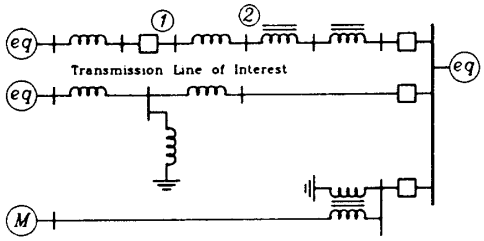

Fig. 6. One-line diagram of system 2.

posed and the long one is not. This should not affect the importance of the results since the algorithms have been developed for untransposed lines.

A number of EMTP simulations of various fault events were performed for testing the proposed algorithms. The initial studies have shown that the algorithms perform best for the largest number of samples. Since the sample window is limited, the largest number of samples is obtained by increasing the sampling frequency. The total time of the simulation was $T_{tot} = 0.032$ s. The data window used in the calculations contained two cycles of postfault data, starting from the fault inception.

The test cases were generated by varying the following four parameters of the fault event: fault location, type of fault, fault resistance, and incidence angle of the fault occurrence.

Each of these simulation parameters was varied within the range of its lower and upper physically meaningful boundaries to provide for the extensive coverage of possible real fault events. Three values for the fault location were considered: 0.1, 0.5, and 0.8, where location 1.0 corresponds to the whole length of the transmission line. Four typical fault types were simulated: single-line to ground (phase a to ground), two-phase (phase b to phase c), two-phase to ground (phase b to phase c to ground), and three-phase to ground. For the fault resistance, values of $R_f = 3\ \Omega$ and $R_f = 50\ \Omega$ were considered, while for the incidence angle, values of 0° and 90° were used.

The error of the fault location algorithms was observed for a variety of fault cases. The error (%) of the fault location algorithm is defined as

$$\text{error (\%)} = \frac{|\text{actual fault loc.} - \text{calculated fault loc.}|}{\text{total line length}} \times 100$$

The results of the test are given in Tables 1–8; the first four tables correspond to the short-line fault location algorithm, the other four to the long-line algorithm. They are organized by the type of fault.

Comparing the error entries related to R_f, it can be seen that the variation in the error is very small. As expected, the algorithms are not affected by the value of the fault resistance R_f. Also, the variation in the incidence angle does not have much influence on the error.

TABLE 1
Error (%) of the short-line fault location algorithm for a phase a to ground fault

Location of fault	0.1		0.5		0.8	
Incidence angle (deg)	0	90	0	90	0	90
$R_f = 3\ \Omega$	0.4344	0.4346	0.2901	0.2093	0.0388	0.0390
$R_f = 50\ \Omega$	0.4576	0.4549	0.2237	0.2229	0.0464	0.0472

TABLE 2
Error (%) of the short-line fault location algorithm for a three-phase to ground fault

Location of fault	0.1		0.5		0.8	
Incidence angle (deg)	0	90	0	90	0	90
$R_f = 3\ \Omega$	0.7084	0.7084	0.3658	0.3658	0.1066	0.1066
$R_f = 50\ \Omega$	0.7084	-0.6991	0.3658	0.3612	0.1066	0.1052

TABLE 3
Error (%) of the short-line fault location algorithm for a phase b to phase c fault

Location of fault	0.1		0.5		0.8	
Incidence angle (deg)	0	90	0	90	0	90
$R_f = 3\Omega$	0.7075	0.7166	0.3658	0.3707	0.1075	0.1091
$R_f = 50\ \Omega$	0.7428	0.7283	0.3915	0.3855	0.1241	0.1262

TABLE 4
Error (%) of the short-line fault location algorithm for a phase b to phase c to ground fault

Location of fault	0.1		0.5		0.8	
Incidence angle (deg)	0	90	0	90	0	90
$R_f = 3\,\Omega$	0.5938	0.5912	0.3159	0.3143	0.0900	0.0885
$R_f = 50\,\Omega$	0.7036	0.7067	0.3635	0.3654	0.1060	0.1066

TABLE 5
Error (%) of the long-line fault location algorithm for a phase a to ground fault

Location of fault	0.1		0.5		0.8	
Incidence angle (deg)	0	90	0	90	0	90
$R_f = 3\,\Omega$	0.4283	0.4212	0.3912	0.3966	0.4783	0.4152
$R_f = 50\,\Omega$	0.4301	0.4832	0.3991	0.4003	0.4853	0.4765

TABLE 6
Error (%) of the long-line fault location algorithm for a three-phase to ground fault

Location of fault	0.1		0.5		0.8	
Incidence angle (deg)	0	90	0	90	0	90
$R_f = 3\,\Omega$	0.6231	0.6734	0.6114	0.6233	0.6723	0.6811
$R_f = 50\,\Omega$	0.6312	0.6846	0.6398	0.6653	0.6942	0.6991

TABLE 7
Error (%) of the long-line fault location algorithm for a phase b to phase c fault

Location of fault	0.1		0.5		0.8	
Incidence angle (deg)	0	90	0	90	0	90
$R_f = 3\,\Omega$	0.7102	0.7098	0.6998	0.7010	0.7306	0.7267
$R_f = 50\,\Omega$	0.7154	0.7135	0.7004	0.7075	0.7388	0.7324

TABLE 8
Error (%) of the long-line fault location algorithm for a phase b to phase c to ground fault

Location of fault	0.1		0.5		0.8	
Incidence angle (deg)	0	90	0	90	0	90
$R_f = 3\,\Omega$	0.4196	0.4087	0.3967	0.3998	0.4325	0.4786
$R_f = 50\,\Omega$	0.4353	0.4144	0.4015	0.4103	0.4587	0.4886

However, for various fault types, the corresponding entries of different tables show a variation in the error magnitude. These observations are equally valid for both the short and the long lines.

When the location of the fault is considered, it was noticed that the error varies less for the long line than for the short one. Further studies are needed to explain this behavior.

Finally, the results indicate that the error is rather small for all cases, as it never exceeds 0.75%. Moreover, typical errors are 0.5% for the most common fault type, namely, the line to ground fault. Such a small error is achieved under varying fault characteristics, which confirms the robustness of the algorithms.

It should also be noted that the computational complexity of the time-domain approach is moderate. Although speed is not a major requirement for the fault location algorithm, it is an important property. The initial studies have shown that the same algorithm can be used for detection and classification of the fault as well. Thus, there are indications that the algorithms could be implemented as a part of a protection device. In that case, the speed of the algorithm becomes very important.

Conclusions

The following conclusions are based on the results presented in this paper.

- The error for the time domain approach presented is almost invariant for the various fault conditions and hence the algorithm provides a robust solution to the fault location problem.
- The new approach improves the accuracy while the computational burden is still kept relatively low.
- The synchronized sampling technique required for this approach is emerging as a reliable and cost-effective practice.

Acknowledgements

The authors wish to acknowledge financial support for Dr. Peruničić and Ms. Mrkić from a NASA grant administered by the Center for Space Power of Texas A&M University. Thanks are also due to Drs. A.D. Patton and F.E. Little from the Center for Space Power for their interest in, and support of, this project.

References

[1] T.W. Springfield, D.J. Marihart and R.F. Stevens, Fault location methods for overhead lines, *Trans. AIEE, Part 3, 76* (1957) 518–530.

[2] E. Born and J. Jaeger, Device locates points of fault on transmission line, *Elect. World, 168* (1967) 133–134.

[3] J. Kohlas, Estimation of fault location on power lines, *Proc. 3rd IFAC Symp., Hague/Delft, Netherlands, 1973*, pp. 393-402.
[4] D.J. Lawrence, L.Z. Cabeza and L.T. Hochbert, Development of an advanced transmission line fault location system, Part II. Algorithm development and simulation, *IEEE Trans. Power Delivery*, 7 (1992) 1972-1983.
[5] L. Eriksson, M.M. Saha and G.D. Rockefeller, An accurate fault location with compensation for apparent reactance in the fault resistance resulting from remote-end infeed, *IEEE Trans. Power Appar. Syst., PAS-104* (1985) 424-435.
[6] T. Takagi, T. Jamakoshi, M. Yamaura, R. Kondow and T. Matshusima, Development of a new type fault locator using one-terminal voltage and current data, *IEEE Trans. Power Appar. Syst., PAS-101* (1982) 2892-2898.
[7] M.S. Sachdev and R. Agarwal, A technique for estimating transmission line fault locations from digital impedance relay measurements, *IEEE Trans. Power Delivery, 3* (1988) 121-129.
[8] A.A. Girgis, D.G. Hart and W.L. Peterson, A new fault location technique for two- and three-terminal lines, *IEEE Trans. Power Delivery*, 7 (1992) 98-107.
[9] A.T. Johns and S. Jamali, Accurate fault location technique for power transmission lines, *Proc. Inst. Electr. Eng., Part C, 137* (1990) 395-401.
[10] T. Takagi, Y. Yamakoshi, J. Baba, K. Uemura and T. Sakaguchi, An algorithm of an accurate fault location for EHV/UHV transmission lines, Part I. Fourier transformation method, *IEEE Trans. Power Appar. Syst., PAS-100* (1981) 1316-1322.
[11] T. Takagi, Y. Yamakoshi, J. Baba, K. Uemura and T. Sakaguchi, A new algorithm of an accurate fault location for EHV/UHV transmission lines, Part II. Laplace transform method, *IEEE Trans. Power Appar. Syst., PAS-101* (1982) 564-573.
[12] Y.G. Paithankar and M.T. Sant, A new algorithm for relaying and fault location based on autocorrelation of traveling waves, *Electr. Power Syst. Res., 8* (1984/85) 179-185.
[13] A.O. Ibe and B.J. Cory, A traveling wave based fault locator for two- and three-terminal networks, *IEEE Trans. Power Delivery, PWRD-1* (1986) 283-288.
[14] A.O. Ibe and B.J. Cory, Fault location algorithm for multiphase power lines, *Proc. Inst. Electr. Eng., Part C, 134* (1987) 43-50.
[15] A.M. Ranjbar, A.R. Shirani and A.F. Fathi, A new approach for fault location problem on power lines, *IEEE Trans. Power Delivery*, 7 (1992) 146-151.
[16] D.J. Lawrence and D.L. Waser, Transmission line fault location using digital fault recorders, *IEEE Trans. Power Delivery, 3* (1988) 496-502.
[17] R.E. Wilson, Methods and uses of precise time in power systems, *IEEE Trans. Power Delivery*, 7 (1992) 126-132.
[18] IEEE Working Group Report, Power System Relaying Committee, Synchronized sampling and phasor measurements for relaying and control, *IEEE Trans. Power Delivery, PWRD-9* (1994) 442-449.
[19] Macrodyne, Inc., Phasor measurement unit—model 1690, *Application Performance Data Sheet*, Clifton Park, NJ, 1993.
[20] Electromagnetic Transient Program (EMTP) Rule Book, *EPRI Project RP 2149-4, Rep. No. EL 6421-I*, Vols. 1 and 2, Electric Power Research Inst., Palo Alto, CA, June 1989.

Appendix A

Bergeron's equations

$$i_S(t-\tau)+\frac{1}{z}v_S(t-\tau)=-i_R(t)+\frac{1}{z}v_R(t) \tag{A1}$$

$$-i_S(t)+\frac{1}{z}v_S(t)=i_R(t-\tau)+\frac{1}{z}v_R(t-\tau) \tag{A2}$$

Modal transform

When the system of coupled wave equations for a three-phase line is written as

$$\frac{\partial \mathbf{v}(x,t)}{\partial x}=-\mathbf{l}\frac{\partial \mathbf{i}(x,t)}{\partial t} \tag{A3}$$

$$\frac{\partial \mathbf{i}(x,t)}{\partial x}=-\mathbf{c}\frac{\partial \mathbf{v}(x,t)}{\partial t} \tag{A4}$$

then the modal transform, defined as

$$\mathbf{v}(x,t)=\mathbf{S}\mathbf{v}^{(\mathrm{mode})}(x,t) \tag{A5}$$

$$\mathbf{i}(x,t)=\mathbf{Q}\mathbf{i}^{(\mathrm{mode})}(x,t) \tag{A6}$$

leads to the decoupled modal equations

$$\frac{\partial \mathbf{v}^{(\mathrm{mode})}(x,t)}{\partial x}=-\mathbf{l}^{(\mathrm{mode})}\frac{\partial \mathbf{i}^{(\mathrm{mode})}(x,t)}{\partial t} \tag{A7}$$

$$\frac{\partial \mathbf{i}^{(\mathrm{mode})}(x,t)}{\partial x}=-\mathbf{c}^{(\mathrm{mode})}\frac{\partial \mathbf{v}^{(\mathrm{mode})}(x,t)}{\partial t} \tag{A8}$$

where $\mathbf{l}^{(\mathrm{mode})}$ and $\mathbf{c}^{(\mathrm{mode})}$ are now diagonal matrices.

Appendix B

TABLE B1
Source impedances (system 1)

Bus name		Per unit value (Ω)	Real value (Ω)
1	Z_0	0.58 + j6.32	1.503 + j16.382
	Z_1	0.58 + j11.41	1.503 + j29.576
2	Z_0	0.07 + j1.07	0.181 + j2.774
	Z_1	0.04 + j0.73	1.104 + j1.892
3	Z_0	0.75 + j4.07	1.944 + j10.550
	Z_1	0.31 + j3.04	0.804 + j7.880

TABLE B2
System equivalents (system 1)

Bus name		Per unit value (Ω)	Real value (Ω)
1-3	Z_0	119.69 + j188.93	310.248 + j489.725
	Z_1	1.80 + j11.44	4.666 + j29.654
1-2	Z_0	∞	∞
	Z_1	12.58 + j74.00	32.609 + j191.815
2-3	Z_0	39.79 + j100.63	103.140 + j260.843
	Z_1	2.75 + j18.32	7.128 + j47.487

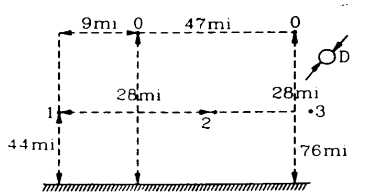

Fig. B1. Long transmission line configuration (system 2).

TABLE B3
Self impedances of transmission lines (system 1)

Bus name		Per unit value (Ω)	Real value (Ω)
1-3 (#1)	Z_0	8.94 + j28.34	23.1734 + j73.4601
	Z_1	1.52 + j9.06	3.9400 + j23.4844
1-3 (#2)	Z_0	8.52 + j29.23	22.0847 + j75.7671
	Z_1	1.38 + j8.80	3.5771 + j76.1300
1-3(#3)	Z_0	8.40 + j29.37	21.7736 + j76.1300
	Z_1	1.34 + j8.73	3.4734 + j22.6290
1-2	Z_0	8.42 + j26.74	21.8255 + j69.3128
	Z_1	1.50 + j8.47	3.8882 + j21.9551
2-3	Z_0	3.67 + j12.38	9.5130 + j32.0902
	Z_1	0.67 + j3.92	1.7367 + j10.1610

TABLE B4
Long transmission line parameters (system 2)

Conductors	Parameters		
	DC resistance (Ω/mile)	Outside diameter D (inches)	Skin effect correction factor
0	3.4400	0.495	0.5000
1	0.0740	1.345	0.2498
2	0.0740	1.345	0.2498
3	0.0740	1.345	0.2498